Oil Shale, 2019, Vol. 36, No. 1, pp. 1–18
doi: https://doi.org/10.3176/oil.2019.1.01
ISSN 0208-189X

AN INVESTIGATION INTO THE CHARACTERISTICS AND KINETICS OF OIL SHALE OXY-FUEL COMBUSTION BY THERMOGRAVIMETRIC ANALYSIS

FENGTIAN BAI[a,b], JINMIN ZHAO[b,c], YUMIN LIU[a,b]*

[a] College of Earth Sciences, Jilin University, Changchun 130061, PR China
[b] Jilin Engineering Research Laboratory for Oil Shale In Situ Pyrolysis and Related Resources Development Technology, Changchun 130021, PR China
[c] Jilin Zhongcheng Oil Shale Group Co., Ltd., Changchun 130000, PR China

Abstract. *The characteristics of Huadian oil shale combustion in O_2/CO_2 atmospheres were compared to those in O_2/N_2 atmospheres by using non-isothermal methods. The combustion kinetics parameters were calculated using the Kissinger-Akahira-Sunose (KAS) and Friedman methods. Specifically, the effect of oxygen concentration (10, 20, 30, 50, 65 and 80% O_2) and heating rate (2, 5, 10 and 20 °C min^{-1}) on the combustion reactivity and kinetics of Huadian oil shale in CO_2-based and N_2-based atmospheres were investigated to identify the optimal gases mixture and oxygen concentration. Comparison of the combustion performances of oil shale in CO_2/O_2 and N_2/O_2 environments indicated that the organic matter combusted earlier in CO_2-based atmospheres than in N_2-based atmospheres when the oxygen concentration was 10% and 20%. Meanwhile, the average activation energies of organic matter combustion in CO_2-based atmospheres was higher than those in N_2-based atmospheres at an oxygen concentration of 10% and 20%. With an appropriate amount of O_2 and CO_2, the combustion performance of oil shale in 30% O_2/70% CO_2 was superior to that in 30% O_2/70% N_2, and the combustion activation energy in the 30% O_2/70% CO_2 atmosphere was also lower. The similar combustion processes and activation energies of oxy-fuel and conventional combustion with oxygen concentrations above 50% indicate that oxygen plays a leading role in organic matter combustion under high oxic conditions. The results reveal that the 30% O_2/70% CO_2 atmosphere is optimal for oil shale combustion.*

Keywords*: oil shale characteristics, thermogravimetric analysis, oxygen concentration, combustion kinetics.*

* Corresponding author: e-mail *csulym@126.com*

1. Introduction

Combustion is the most simple and direct technology currently available for oil shale utilization [1]. However, growing concerns regarding CO_2, SO_2, and NO_x emissions and their potential impact on climate change have necessitated the investigation of alternative technologies for oil shale-fired power plants.

Oxy-fuel combustion is an innovative and promising clean combustion technology that can be used to capture cheap CO_2 from flue gases at concentrations enriched up to 95% [2–4]. The gas atmosphere in oxy-fuel combustion differs completely from that in conventional combustion. This is because the special property of CO_2 is that it has a higher specific heat and lower thermal diffusivity compared to those of N_2 and the mass transport of O_2 to and through the reacting particles changes owing to the differences in its mass diffusivity between CO_2 and N_2 [3]. Thus, the combustion and kinetic characteristics of solid fuels in oxy-fuel combustion are of interest in fuel research [3–11].

However, only a few researches have been conducted into the combustion behavior of oil shale in oxy-fuel conditions using the thermogravimetric (TG) method. Jabber and Probert [8] reported that there was a slightly greater mass loss during the devolatilization of Jordanian oil shale in CO_2 than in N_2, and that the CO_2-char reaction was more likely to occur at high temperatures. Meriste et al. [9] compared the oxidation kinetics of oil shale and coal in 79% Ar/21% O_2 and 70% CO_2/30% O_2. Yörük et al. [10] showed that the pyrolysis behavior of Estonian oil shale was very similar in Ar and CO_2 during water evaporation and organic matter decomposition, and the rate constants for char oxidation in O_2/CO_2 were approximately 1.2–1.3-times higher than those in the O_2/Ar atmosphere. Additionally, Loo et al. [11] studied the combustion behavior of Estonian oil shale in O_2/N_2 and O_2/CO_2 environments with different oxygen concentrations (10, 20 and 30%), and found that the carbonate minerals in oil shale decomposed in one step in O_2/N_2 and in two separate steps in O_2/CO_2, but their kinetic characteristics were not investigated.

The combustion behavior of Huadian oil shale in the atmosphere of O_2/N_2 of different concentrations has been studied by Bai et al. [12]. The researchers found that the combustion performance of oil shale could be significantly improved with an increase in oxygen concentration from 10 to 50%. Xie et al. [13] investigated the pyrolytic behavior of Huadian oil shale in N_2 and CO_2 atmospheres and discovered that the carrier gas did not change the mass loss or the mechanism of devolatilization of organic matter, while the decomposition of carbonate minerals could be retarded by CO_2. Nevertheless, the combustion reactivity and kinetics of Huadian oil shale under oxy-fuel conditions have not yet been thoroughly explored. More researches are needed to fully understand the oxy-fuel combustion process of Huadian oil shale and its reaction kinetics.

In the present study, the characteristics of oil shale combustion in O2/CO2 atmospheres are compared to those in O_2/N_2 atmospheres by using non-isothermal methods. The effect of oxygen concentration and heating rate on the oil shale combustion are also studied. In addition, Kissinger-Akahira-Sunose (KAS) and Friedman methods are applied to determine the kinetic parameters of the combustion process.

2. Experimental

2.1. Material

Samples of Huadian oil shale, China were selected for this study. Raw oil shale samples were ground and sieved to a grain size less than 88 μm and dried at 45–50 °C for 24 hours before experiment. The physical properties of oil shale are presented in Table 1.

Table 1. Physical properties of Huadian oil shale

Proximate analysis, wt%, ad		Ultimate analysis, wt%, ad		Fischer assay analysis, wt%, ad	
Volatiles	39.34	C	28.55	Shale oil	19.69
Fixed carbon	3.75	H	3.58	Gas + Loss	6.38
Ash	56.91	N	0.65	Water	4.98
Moisture (as received)	3.26	S	1.34	Residue	68.95
Calorific value, MJ kg^{-1}	13.07				

Note: ad = air-dried.

2.2. Thermogravimetric analysis

The TG analysis experiments were carried out on a Netzsch STA 449C thermal analyzer system. The samples were heated up to 850 °C at the heating rates of 2, 5, 10 and 20 °C min^{-1} in both CO_2-based and N_2-based atmospheres with 10, 20, 30, 50, 65 and 80% O_2. Repeated experiments were performed to ensure the reproducibility.

2.3. Characteristic parameters and combustion reactivity

Ignition temperature (T_i), maximum mass loss rate temperature (T_{max}) and burnout temperature (T_b) were used to describe the thermal behavior of oil shale during combustion.

The combustion reactivity index, R, is expressed as [14]:

$$R = -\frac{1}{m - m_\infty}\frac{dm}{dt} = \frac{1}{1-\alpha}\frac{d\alpha}{dt}, \quad (1)$$

where $\alpha = (m_0 - m)/(m_0 - m_\infty)$ is the conversion fraction obtained from the TG/derivative thermogravimetric (DTG) curves, m_0, m_∞ and m represent the

initial, final and instantaneous mass of the sample, respectively, and $d\alpha/dt$ is the conversion rate. The combustion reactivity is dependent on the solid-fuel conversion. In this study, the combustion reactivities at both 5% conversion (R_5) and 50% conversion (R_{50}) were used to evaluate the combustion performance of oil shale.

The product release index, r [15], which reflects the product release intensity during combustion, is expressed as:

$$r = \frac{(dw/dt)_{\max}}{T_{\max} \cdot T_i \cdot \Delta T_{1/2}}, \tag{2}$$

where $(dw/dt)_{\max}$ is the maximum mass loss rate, % min^{-1}, and $\triangle T_{1/2}$ is the temperature range of the half-peak, °C. Generally, the high product release index r means that during the process an intensive release of products takes place.

2.4. Kinetic method

In this study, the activation energies were determined from experiments at heating rates of 2, 5, 10 and 20 °C min^{-1} by using KAS and Friedman methods.

The general kinetic equation is usually defined as:

$$\frac{d\alpha}{dt} = \mathrm{k}\, f(\alpha) \quad \text{or} \quad \frac{d\alpha}{dT} = \frac{A}{\beta}\exp\left(-\frac{E}{R_c T}\right) f(\alpha), \tag{3}$$

where $d\alpha/dt$ is the conversion rate, k is the rate constant, $f(\alpha)$ is the kinetic model function, A is the pre-exponent factor, min^{-1}, E is the activation energy, kJ mol^{-1}, β is the heating rate, °C min^{-1}, and R_c is the universal gas constant, 8.314 J mol^{-1} K^{-1}.

The KAS equation [16] is given as:

$$\ln\left(\frac{\beta}{T^2}\right) = \ln\left(\frac{AR_c}{EG(\alpha)}\right) - \frac{E}{R_c T}, \tag{4}$$

where $G(\alpha)$ is the integral form of $f(\alpha)$.

The equation for the Friedman method [17] is:

$$\ln\left(\beta\frac{d\alpha}{dT}\right) = \ln\left[Af(\alpha)\right] - \frac{E}{R_c T}. \tag{5}$$

Under the conversion at different temperatures and heating rates, the regression lines of $\ln(\beta/T^2)$ vs $1/T$ for the KAS method and $\ln\left(\beta\frac{d\alpha}{dT}\right)$ vs $1/T$ for the Friedman method provide an estimate of activation energy from the slope.

3. Results and discussion

3.1. TG study

3.1.1. Combustion characteristics in O_2/CO_2 and O_2/N_2 atmospheres

According to the TG results, the main stages of oil shale combustion are water evaporation (below 200 °C), organic matter combustion (200–600 °C) and inorganic matter decomposition (above 650 °C) for both CO_2-based and N_2-based atmospheres. As shown in Figure 1, the combustion behavior of oil shale is dissimilar at different proportions of CO_2 and N_2, especially above 250 °C in the atmosphere of high CO_2/N_2 concentrations, which indicates that CO_2 and N_2 have a different influence on the combustion of organic matter. Figure 2a shows that at a constant volume of CO_2 its density and specific heat are both higher than those of N_2 at a temperature of 200–700 °C. At the same time, with increasing temperature, the specific heat of CO_2 at constant pressure and its thermal conductivity become higher compared with those of N_2. The differences in physical properties between CO_2 and N_2 are the major reason for the disparities between the combustions in O_2/CO_2 and O_2/N_2. The differences in specific heat and thermal conductivity between CO_2 and N_2 lead to the different gas heat transfer process. In addition, the mass transport process of O_2 to and through the reacting particles is also different due to the differences in the mass diffusivity of oxygen through the diluent gas [3]. Figure 2b shows that the differences in density, specific heat, thermal conductivity and thermal diffusivity between O_2/CO_2 and O_2/N_2 atmospheres decrease with the oxygen concentration increasing from 10 to 80%.

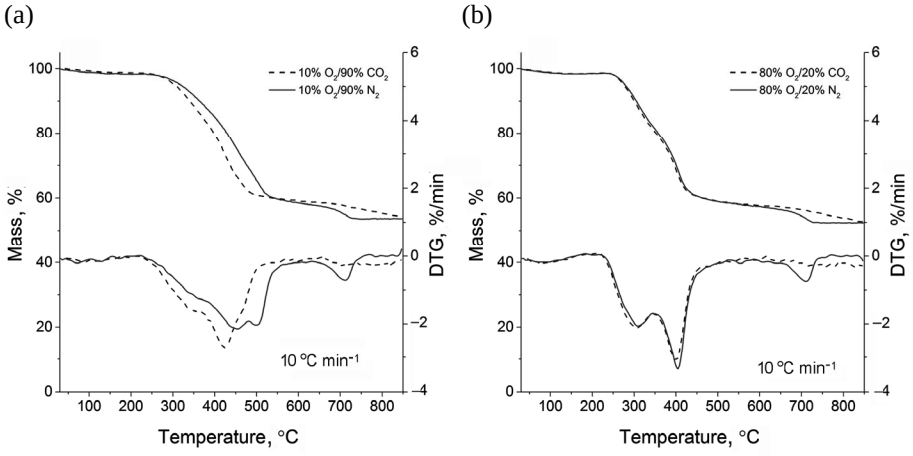

Fig. 1. TG and DTG curves of Huadian oil shale in: (a) 10% O_2/90% CO_2 and 10% O_2/90% N_2 and (b) 80% O_2/20% CO_2 and 80% O_2/20% N_2 atmospheres.

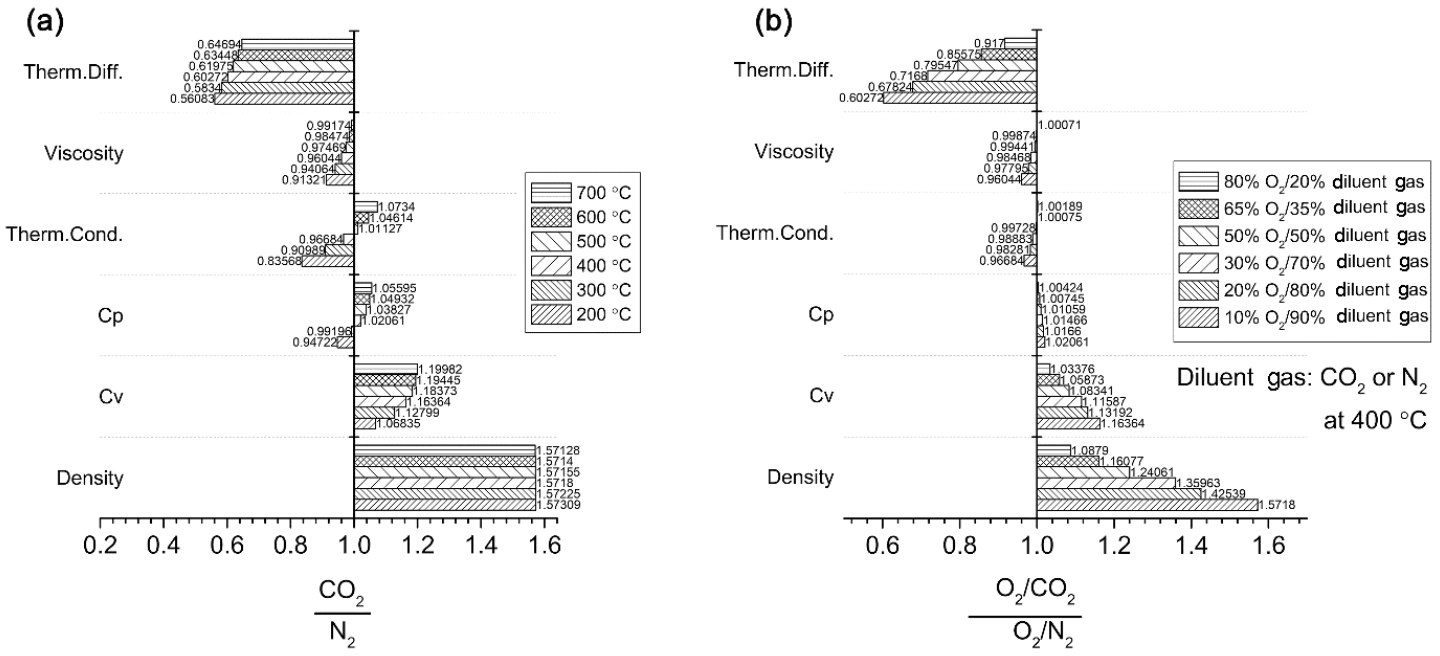

Fig. 2. Comparison of the ratios of different physical properties: (a) for CO_2 and N_2, (b) for O_2/CO_2 and O_2/N_2 at 0.1 MPa. (The abbreviations used: Therm. Diff. – thermal diffusivity; Therm. Cond. – thermal conductivity; Cp – specific heat at constant pressure; Cv - specific heat at constant volume.)

With 10% O_2, the organic matter combusted earlier and in narrower temperature ranges in CO_2-based atmospheres than in N_2-based atmospheres. Furthermore, there are two strong peaks in DTG curves, one between 230 and 390 °C and the other in the range of 390–500 °C in CO_2-based atmospheres, and at 230–480 °C and 480–550 °C in N_2-based atmospheres (Fig. 1a). The T_{max} in 10% O_2/90% CO_2 is 423 °C and 454 °C in 10% O_2/90% N_2. The combustion reactivity in 10% O_2/90% CO_2, as indicated by the combustion reactivity indices (R_5 and R_{50}) and product release index (r), is higher than that in the 10% O_2/90% N_2 atmosphere (Table 2), which is primarily due to the differences in physical and thermal properties, such as density, specific heat and thermal conductivity, between the gas atmospheres [3, 10]. The gasification reaction between CO_2 and fixed carbon may occur earlier at a high concentration of CO_2. This also means that longer residence times or higher temperatures are needed for oxidation of oil shale in N_2-based atmospheres than in CO_2-based atmospheres whose oxygen concentration is low.

With 80% O_2, the combustion behavior of oil shale in CO_2-based and N_2-based atmospheres is very similar up to 550 °C. The T_{max} of organic matter combustion is at around 400 °C in both the atmospheres. The combustion reactivity in 20% CO_2 is slightly lower than that in 20% N_2. There is no significant mass loss difference until the end of organic devolatilization, and the TG curves for the oil shale samples in 80% O_2/20% CO_2 and 80% O_2/20% N_2 are almost superimposable. This indicates that when the oxygen concentration increases to some extent, the effect of the diluent gas on the physical and chemical processes of combustion becomes negligible (Fig. 2b).

When the temperature increases above 650 °C, the endothermic decomposition of carbonates in oil shale proceeds in one step at 650–750 °C in N_2-based atmospheres, while there is a slow and continuous decrease in the process intensity from 650 °C to 850 °C in CO_2-based environements, as TG curves show (Fig. 1a, 1b). This may be because the char formed during the organic combustion process is gasified by CO_2. At the same time, the carbonates decomposition may be delayed in CO_2-based atmospheres. Xie et al. [13] observed an obvious delay in the decomposition of mineral carbonates in Huadian oil shale in CO_2-based atmospheres when the temperature was above 700 °C. Estonian oil shale undergoes two reaction steps in oxy-fuel conditions above 650 °C, the first in the 650–890 °C range and the second between 890 and 960 °C [9–11]. Furthermore, Yörük et al. [10] reported that the decomposition temperatures of $MgCO_3$ and $CaCO_3$ in CO_2 were different and the processes proceeded with maximum rates at 750 °C and 920 °C, respectively. The different properties of oil shale (especially the composition of shale ash) and the reactivity of char may have different influences on carbonates decomposition and the char-CO_2 reaction during the gasification process. Furthermore, the maximum experimental temperature (850 °C) used in this study also influenced the entire decomposition processes of carbonates.

Table 2. Characteristic parameters of combustion of Huadian oil shale organic matter in O_2/CO_2 and O_2/N_2 atmospheres

Atmosphere	β, °C min^{-1}	$(dw/dt)_{max}$, % min^{-1}	T_{max}, °C	T_i, °C	T_b, °C	$\triangle T_{1/2}$, °C	$r(\times 10^{-7})$	R_5	R_{50}
10% O_2/90% CO_2	10	–2.77	423.1	281.3	470.0	150.3	1.5485	0.0010	0.0098
20% O_2/80% CO_2	10	–3.06	414.6	273.3	456.5	137.4	1.9655	0.0015	0.0106
30% O_2/70% CO_2	2	–0.76	377.5	237.9	394.7	130.7	0.6475	0.0023	0.0084
	5	–1.92	397.5	252.2	418.7	125.2	1.5297	0.0016	0.0096
	10	–3.30	416.6	263.8	449.7	137.8	2.1791	0.0022	0.0097
	20	–5.41	435.5	277.6	495.2	176.6	2.5340	0.0013	0.0102
50% O_2/50% CO_2	10	–3.35	407.7	256.1	433.2	137.2	2.3385	0.0022	0.0096
65% O_2/35% CO_2	10	–3.41	404.9	252.2	426.2	140.2	2.3818	0.0025	0.0091
80% O_2/20% CO_2	10	–3.42	400.2	249.0	421.8	139.9	2.4532	0.0018	0.0095
10% O_2/90% N_2	10	–2.15	454.1	286.4	525.8	187.7	0.8807	0.0009	0.0087
20% O_2/80% N_2	10	–2.87	422.9	270.9	483.5	150.0	1.6701	0.0010	0.0103
30% O_2/70% N_2	2	–0.80	377.4	241.1	395.9	113.8	0.7726	0.0014	0.0103
	5	–1.84	400.2	262.2	421.6	122.0	1.4373	0.0014	0.0108
	10	–3.08	416.7	272.6	460.4	138.5	1.9577	0.0016	0.0119
	20	–4.95	436.9	284.7	501.7	178.4	2.2307	0.0010	0.0100
50% O_2/50% N_2	10	–3.26	408.3	264.2	438.0	135.6	2.2287	0.0016	0.0097
65% O_2/35% N_2	10	–3.32	406.5	261.2	429.4	135.8	2.3025	0.0018	0.0098
80% O_2/20% N_2	10	–3.33	404.0	255.3	429.1	139.6	2.3127	0.0020	0.0096

3.1.2. Effects of oxygen concentration and heating rate

The combustion performance of oil shale at various concentrations of CO_2 and N_2 was determined at a heating rate of 10 °C min^{-1} (Fig. 3). A higher oxygen concentration in both CO_2-based and N_2-based atmospheres leads to a faster combustion of organic matter, while T_{max} and T_b of organic matter combustion decrease with increasing oxygen concentrations, especially from 10 to 50%. The effect is stronger in N_2 than in CO_2. This may be because the diffusivity of O_2 in N_2 is stronger than that in CO_2, which improves the transport of O_2 from the mixture gas to the oil shale particle surfaces. Moreover, the combustion in the CO_2 atmosphere is more intense than that in N_2 when the oxygen concentration is low.

The product release index (r) increases as the oxygen concentration increases in both CO_2-based and N_2-based atmospheres, which indicates that the products are formed intensively at high oxygen concentrations. This is consistent with the results reported by Bai et al. [12]. The combustion reactivity indices R_5 and R_{50} first increase and then decrease when the oxygen concentration in CO_2-based atmospheres is increased, reaching their maximum values at an oxygen concentration of 65% and 20%, respectively. In N_2-based atmospheres, R_5 rises with increasing oxygen concentration, while R_{50} reaches its maximum value when the oxygen concentration is about 30%. Consequently, the oil shale combustion performance can be greatly enhanced by increasing the oxygen concentration, but this improvement becomes less considerable when the oxygen concentration is beyond a certain concentration [12]. Moreover, R_5 in CO_2-based atmospheres is increased slightly less than that in N_2-based atmospheres (except for the oxygen concentration of 80%). The R_{50} values in CO_2-based

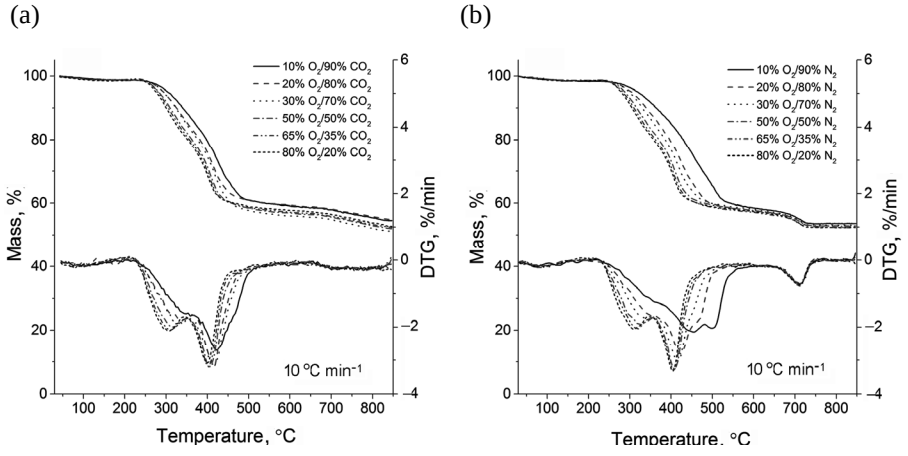

Fig. 3. TG and DTG curves of Huadian oil shale combustion at different concentrations of (a) O_2/CO_2 and (b) O_2/N_2.

atmospheres are lower than those in N_2-based atmospheres except for oxygen concentrations of 10% and 20%. The higher specific heat and lower diffusivity of CO_2 compared to those of N_2 worsen the transport of O_2 from the mixture gas to the oil shale particle surfaces and reduce the oil shale combustion rate in oxy-fuel conditions at high temperatures at high oxygen concentrations. The heat release process is slightly less vigorouslower than the combustion process during TG tests.

The oxygen concentration has almost no influence on the decomposition of inorganic matter in the O_2/N_2 mixture. This is in agreement with the results obtained by Loo et al. [11]. However, the maximum experimental temperature in the current study made it impossible to analyze the influence of oxygen concentration on the mineral decomposition in the O_2/CO_2 atmosphere. Loo et al. [11] found that a higher oxygen concentration could reduce the characteristic temperatures of the second stage of the combustion process, but had little influence on carbonates decomposition. Furthermore, there were no obvious differences in the total mass losses of oil shale between CO_2-based and N_2-based atmospheres in the studied temperature range.

Figure 4 shows the TG and DTG curves of the combustion process of samples at heating rates of 2, 5, 10 and 20 °C min^{-1} at an oxygen concentration of 30%. As seen from Figure 4 and Table 2, the combustion processes are clearly affected by the heating rates in both CO_2-based and N_2-based atmospheres. The characteristic temperatures T_i, T_{max}, T_b and the product release index (r) in the organic matter combustion stage increases as the heating rate increases in both atmospheres, indicating that there exists thermal hysteresis if heating rates are high [18]. For low heating rates with a long combustion time, the reaction proceeds more vigorously and the mass

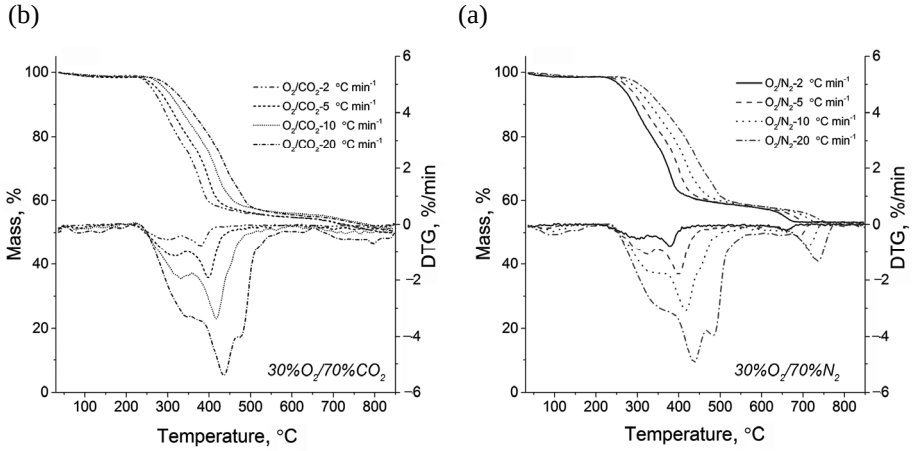

Fig. 4. TG and DTG curves of Huadian oil shale combustion at different heating rates in: (a) 30% O_2/70% CO_2 and (b) 30% O_2/70% N_2.

loss occurs in a narrower temperature range due to a homogenous temperature distribution within the oil shale particles, while the release of products is rapid and intensive as a result of a short combustion time at high heating rates [12]. At the same time, there is no certain relationship between the combustion reactivity indices (R_5 and R_{50}) and heating rates. The R_5 values in O_2/CO_2 atmospheres are slightly higher than those in O_2/N_2 atmospheres. The R_{50} values in O_2/CO_2 environments are lower than those in O_2/N_2, except at a heating rate of 20 °C min^{-1}.

3.2. Kinetic analysis

The calculated activation energies are given in Tables 3 and 4. The activation energies determined by the Friedman method are slightly higher than those obtained by the KAS method for both CO_2-based and N_2-based atmospheres. This deviation is attributed to the discrepancy in equation parameters, numerical differentiations and model assumptions [19], and is also consistent with the results of other researches [12, 18, 20]. From Tables 3 and 4 it can be seen that the activation energy values fluctuate significantly. If α is 0.1 or 0.9, especially in oxy-fuel combustion, the lower R^2 value indicates that the reaction is unstable during the initial and end periods of oil shale combustion.

The decrease of activation energy in the initial period of combustion reveals that at this stage the process is rather complex and proceeds slowly [9]. After exceeding the threshold energy, the product changes into a reactant and combusts, after which the whole process proceeds more rapidly [12]. The fluctuating activation energies for organic matter combustion at α = 0.2–0.8, particularly for oxy-fuel combustion, are mainly in relation to the two DTG peaks [12, 21]. At the same time, different components are burned during low-temperature and high-temperature oxidation periods, while macromolecular non-volatiles and inert components are burned at a higher temperature, which hinders the mass transfer and decreases the combustion reactivity, as a result, the activation energy increases [12, 21, 22]. When the conversion rate exceeds 0.9, a high energy is needed for inorganic matter decomposition [9].

For CO_2-based atmospheres, the activation energy values for organic matter combustion markedly decline, from 90.2 to 73.6 kJ mol^{-1}, when using the KAS method, and from 100.6 to 80.6 kJ mol^{-1} by using the Friedman method, with α = 0.2–0.8 and the oxygen concentration of 10%. With increasing oxygen concentration, the activation energy at α = 0.2–0.8 first decreases until α = 0.4 and then increases up to α = 0.7, after which it decreases again. The kinetics of oil shale combustion in the atmosphere of O_2/N_2 of different concentrations has been discussed in more detail by Bai et al. [12]. The researchers employed heating rates of 5, 10 and 20 °C min^{-1} and calculated activation energies. The E values

Table 3. Kinetic parameters of oil shale oxy-fuel combustion in the O_2/CO_2 atmosphere

Method	α	10% O_2/90% CO_2		20% O_2/80% CO_2		30% O_2/70% CO_2		50% O_2/50% CO_2		65% O_2/35% CO_2		80% O_2/20% CO_2	
		E, kJ mol^{-1}	R^2	E, kJ mol^{-1}	R^2	E, kJ mol^{-1}	R^2	E, kJ mol^{-1}	R^2	E. kJ mol–^{1}	R^2	E, kJ mol^{-1}	R^2
KAS	0.1	115.2	0.9654	107.3	0.9961	112.1	0.9777	132.8	0.9916	127.7	0.9922	156.0	0.9870
	0.2	90.2	0.9799	103.6	0.9969	99.7	0.9882	115.8	0.9950	122.3	0.9965	135.4	0.9897
	0.3	79.4	0.9819	95.9	0.9979	90.7	0.9908	108.2	0.9980	111.2	0.9966	123.3	0.9922
	0.4	78.2	0.9829	96.3	0.9991	89.6	0.9954	100.9	0.9995	103.1	0.9974	111.5	0.9930
	0.5	81.7	0.9800	106.5	0.9994	99.4	0.9958	108.4	1.0000	112.2	0.9999	115.8	0.9972
	0.6	79.7	0.9681	116.3	0.9970	105.9	0.9940	125.7	0.9999	128.9	0.9999	133.4	0.9973
	0.7	73.2	0.9595	113.2	0.9882	101.0	0.9824	132.1	0.9988	137.9	0.9986	145.0	0.9960
	0.8	73.6	0.9826	130.5	0.9537	96.8	0.9890	120.7	0.9943	130.1	0.9923	136.8	0.9605
	0.9	305.5	0.9118	259.1	0.7741	267.7	0.7946	258.2	0.6078	266.4	0.5486	248.1	0.8929
	Average[a]	79.4		108.9		97.6		116.0		120.8		128.7	
Friedman	0.1	125.1	0.9706	116.9	0.9968	121.8	0.9811	142.4	0.9928	137.3	0.9933	165.6	0.9885
	0.2	100.6	0.9841	113.7	0.9975	109.8	0.9904	125.8	0.9959	132.2	0.9971	145.3	0.9911
	0.3	90.2	0.9863	106.3	0.9984	101.2	0.9928	118.5	0.9984	121.4	0.9973	133.5	0.9934
	0.4	89.3	0.9873	107.2	0.9993	100.5	0.9965	111.5	0.9996	113.7	0.9980	122.1	0.9943
	0.5	93.3	0.9851	117.8	0.9996	110.7	0.9968	119.5	1.0000	123.3	0.9999	126.8	0.9978
	0.6	91.5	0.9763	127.9	0.9976	117.5	0.9953	137.1	0.9999	140.4	1.0000	144.8	0.9978
	0.7	85.3	0.9708	125.1	0.9905	112.9	0.9862	143.9	0.9991	149.6	0.9989	156.7	0.9967
	0.8	86.1	0.9879	142.9	0.9613	109.0	0.9916	132.8	0.9954	142.2	0.9936	148.8	0.9665
	0.9	321.0	0.9189	265.2	0.7531	281.4	0.7923	272.9	0.6122	282.8	0.5762	266.6	0.8827
	Average[a]	90.9		120.1		108.8		127.0		131.8		139.7	

[a] Average energy if α = 0.2–0.8.

Table 4. Kinetic parameters of oil shale combustion in the O_2/N_2 atmosphere

Method	α	10% O_2/90% N_2		20% O_2/80% N_2		30% O_2/70% N_2		50% O_2/50% N_2		65% O_2/35% N_2		80% O_2/20% N_2	
		E, kJ mol^{-1}	R^2	E, kJ mol^{-1}	R^2	E, kJ mol^{-1}	R^2	E, kJ mol^{-1}	R^2	E, kJ mol^{-1}	R^2	E, kJ mol^{-1}	R^2
KAS	0.1	92	0.9696	104.93	0.9797	114.25	0.9918	125.9	0.9954	126.5	0.9796	125.1	0.9884
	0.2	75.67	0.9774	92.47	0.9865	104.85	0.9922	118.1	0.9970	123.5	0.9899	125.6	0.9926
	0.3	66.57	0.9801	83.97	0.9833	96.25	0.9939	108.4	0.9985	111.8	0.9929	118.1	0.9966
	0.4	66.6	0.9861	84.33	0.9865	95.5	0.9970	102.6	0.9994	105.8	0.9975	109.7	0.9988
	0.5	65.4	0.9748	90.93	0.9767	104.15	0.9971	112.2	0.9990	116.2	0.9994	117.5	0.9992
	0.6	59.87	0.9552	92.6	0.9604	112.75	0.9916	125.8	0.9996	130.1	0.9998	134.6	0.9989
	0.7	54.13	0.9506	84.67	0.9594	107.7	0.9804	129.0	0.9962	132.4	0.9968	142.8	0.9986
	0.8	54.23	0.9352	87.57	0.9778	106.55	0.9903	117.9	0.9984	122.1	0.9956	133.7	0.9988
	0.9	199.87	0.8971	307.67	0.9750	282.95	0.9273	277.9	0.9681	258.9	0.9882	227.7	0.7350
	Average[a]	63.2		88.1		104.0		116.3		120.3		126.0	
Friedman	0.1	102	0.9757	114.67	0.9832	123.95	0.9932	135.5	0.9961	137.5	0.9825	134.6	0.9900
	0.2	86.2	0.9834	102.73	0.9895	115	0.9938	128.2	0.9975	132.8	0.9916	137.4	0.9938
	0.3	77.63	0.9863	94.63	0.9877	106.75	0.9953	118.7	0.9989	121.7	0.9942	130.3	0.9973
	0.4	77.97	0.9908	95.3	0.9902	106.3	0.9978	113.3	0.9995	117.3	0.9980	122.2	0.9991
	0.5	77.27	0.9835	102.33	0.9828	115.4	0.9978	123.3	0.9991	126.9	0.9995	130.1	0.9992
	0.6	72.1	0.9720	104.37	0.9709	124.4	0.9935	137.3	0.9997	141.3	0.9998	130.3	0.9992
	0.7	66.67	0.9712	96.67	0.9712	119.55	0.9850	140.7	0.9969	145.1	0.9974	156	0.9989
	0.8	67.2	0.9630	99.93	0.9845	118.8	0.9927	130.0	0.9987	134.2	0.9965	147.2	0.9990
	0.9	215.13	0.9153	323.27	0.9769	298.55	0.9336	293.3	0.9710	263.3	0.9894	242.9	0.7579
	Average[a]	75.0		99.4		115.2		127.4		131.3		136.2	

[a] Average energy if α = 0.2–0.8.

obtained in the current study comply with the data reported by Bai et al. earlier [12]. As seen from Figure 5 and Tables 3 and 4, the average activation energy at α = 0.2–0.8 for both CO_2-based and N_2-based atmospheres increases with increasing oxygen concentration, except for 30% O_2/70% CO_2. The activation energy of oil shale is influenced by the concentration of activated molecules, diffusion limitation and organic impurities present in the combustion process [5, 22, 23]. An increase in the oxygen ratio can enhance the oxidation of kerogen and accelerate the decomposition of inorganic matter, making the reaction more intense [11] and increasing the activation energy.

As shown in Figure 5, the average activation energies of organic matter combustion in CO_2-based atmospheres are higher than those in N_2-based environments when the oxygen concentration is 10% and 20%. This indicates that the dissimilarity between CO_2-based and N_2-based atmospheres cannot be neglected if oxygen concentrations are low. The physical and thermal parameters of CO_2, such as density, specific heat at constant volume and thermal conductivity, are all higher than those of N_2 to various degrees at temperatures up to 400 °C (Fig. 2a), which leads to a delay in the increase of the temperature of gas and fuel particles under CO_2-based conditions [3]. This may diminish the thermal hysteresis and the temperature gradient in the shale particles, allowing the reaction to proceed more homogeneously and intensively and making the product generation and diffusion more balanced in CO_2-based atmospheres. In addition, the carbon gasification catalyzed by the mineral matter in oil shale [8, 24, 25] takes place between CO_2 and semi-coke/fixed carbon during the devolatilization process at high CO_2 concentrations [11], which can improve the pore structure and particle diffusion. Therefore, the organic matter combusts quickly and numerous

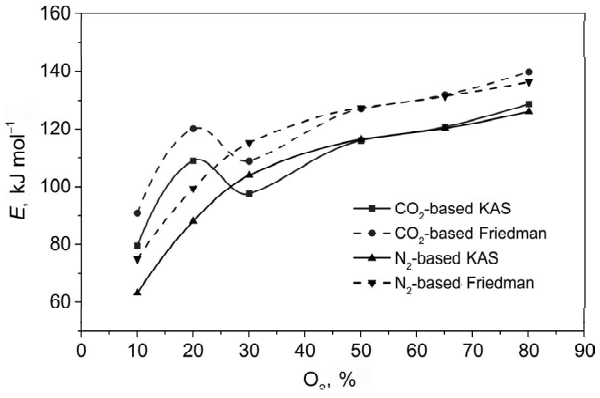

Fig. 5. Average activation energies for organic matter combustion at different oxygen concentrations.

complex reactive processes occur simultaneously in high-concentration CO_2 atmospheres as seen from Figure 1a, thus increasing the activation energy in these atmospheres.

For 30% O_2/70% CO_2, more active reaction sites appear to promote organic matter combustion by the elevated oxygen level, and, meanwhile, the pore and surface areas are increased due to the CO_2-char reaction [26]. Consequently, the combustion activation energies in 30% O_2/70% CO_2 are lower than those in the 30% O_2/70% N_2 atmosphere. The negligible difference in activation energy between CO_2-based and N_2-based environments with oxygen concentrations above 50% indicates that the element plays a leading role in organic matter combustion at high concentrations, while at concentrations above 50% its contribution to improving the combustion process does not increase [12]. Al-Makhadmeh et al. [27, 28] studied the oxy-fuel combustion of oil shale by using a 20 kW once-through furnace, and found that SO_2 and NO_X emissions under oxy-fuel conditions were lower than those in conventional combustion when the oxygen concentration was about 30%. Considering the cost, the improvement of combustion behavior by further oxygen enrichment above 50% may not be justified. An oxygen concentration of 30% may be the best choice, especially for the 30% O_2/70% CO_2 atmosphere.

4. Conclusions

The combustion and kinetics characteristics of Huadian oil shale at various oxygen concentrations have been investigated by thermogravimetry. The combustion kinetic parameters have been calculated using the Kissinger-Akahira-Sunose and Friedman methods. An increase in the oxygen ratio in the atmospheres studied can enhance the oxidation of kerogen and accelerate the decomposition of inorganic matter, making the reaction more intense, especially for N_2-based atmospheres, simultaneously increasing the activation energy, except for 30% O_2/70% CO_2. However, the improvement of combustion properties from further oxygen enrichment decrease sharply above the 50% oxygen concentration. Comparison of oil shale combustion processes in CO_2/O_2 and N_2/O_2 atmospheres with the oxygen concentrations of 10% and 20% indicate that organic matter combusts earlier and more vigorously in CO_2-based mixtures than in N_2-based atmospheres. This leads to higher average activation energies of organic matter combustion in CO_2-based environments than in N_2-based atmospheres. This is due to the different physical and thermal parameters of CO_2 and N_2. With more active reaction sites appearing because of the increased oxygen concentration as well as increased pore and surface areas due to the CO_2-char reaction, the activation energies in 30% O_2/70% CO_2 are lower than those in the 30% O_2/70% N_2 atmosphere. That difference of diluent gas decreases as the oxygen concentration increases above 50%, moreover, similar thermo-

gravimetry curves, combustion performances and activation energies for oxy-fuel and conventional combustions at oxygen concentrations above 50% indicate that the element plays a leading role in organic matter combustion. For the better combustion performance and lower activation energies, an oxy-fuel combustion in 30% O_2/70% CO_2 may be the best choice for oil shale combustion. Moreover, the behaviour of oil shale in the oxy-fuel combustion is similar to that in air (20% O_2/80% N_2), which eases the design of oxy-fuel combustors.

Acknowledgements

This work was supported by the National Natural Science Foundation of China (Grant No.51604123) and the Science and Technology Project of the Department of Jilin Province, China (Grant Nos. 20170201001SF, 20180201077SF, 20190103138JH).

REFERENCES

1. Özgür, E., Miller, S. F., Miller, B. G.., Kök, M. V. Thermal analysis of co-firing of oil shale and biomass fuels. *Oil Shale*, 2012, **29**(2), 190–201.
2. Toftegaard, M. B., Brix, J., Jensen, P. A., Glarborg, P., Jensen, A. D. Oxy-fuel combustion of solid fuels. *Prog. Energ. Combust*., 2010, **36**(5), 581–625.
3. Wang, C. A., Zhang, X. M., Liu, Y. H., Che, D. F. Pyrolysis and combustion characteristics of coals in oxyfuel combustion. *Appl. Energ*., 2012, **97**, 264–273.
4. Yuzbasi, N. S., Selçuk, N. Air and oxy-fuel combustion characteristics of biomass/lignite blends in TGA-FTIR. *Fuel Process. Technol*., 2011, **92**(5), 1101–1108.
5. Chen, C. X., Lu, Z. G., Ma, X. Q., Long, J., Peng, Y. N., Hu, L. K., Lu, Q. Oxy-fuel combustion characteristics and kinetics of microalgae *Chlorella vulgaris* by thermogravimetric analysis. *Bioresource Technol*., 2013, **144**, 563–571.
6. López, R., Fernández, C., Fierro, J., Cara, J., Martínez, O., Sánchez, M. E. Oxy-combustion of corn, sunflower, rape and microalgae bioresidues and their blends from the perspective of thermogravimetric analysis. *Energy*, 2014, **74**, 845–854.
7. Meng, F., Yu, J., Tahmasebi, A., Han, Y. Pyrolysis and combustion behavior of coal gangue in O_2/CO_2 and O_2/N_2 mixtures using thermogravimetric analysis and a drop tube furnace. *Energ. Fuel*., 2013, **27**(6), 2923–2932.
8. Jaber, J. O., Probert, S. D. Pyrolysis and gasification kinetics of Jordanian oil-shales. *Appl. Energ*., 1999, **63**(4), 269–286.
9. Meriste, T., Yörük, C. R., Trikkel, A., Kaljuvee, T., Kuusik, R. TG-FTIR analysis of oxidation kinetics of some solid fuels under oxy-fuel conditions. *J. Therm. Anal. Calorim*., 2013, **114**(2), 483–489.
10. Yörük, C. R., Meriste, T., Trikkel, A., Kuusik, R. Thermo-oxidation characteristics of oil shale and oil shale char under oxy-fuel combustion conditions. *J. Therm. Anal. Calorim*., 2015, **121**(1), 509–516.

11. Loo, L., Maaten, B., Siirde, A., Pihu, T., Konist, A. Experimental analysis of the combustion characteristics of Estonian oil shale in air and oxy-fuel atmospheres. *Fuel Process. Technol.*, 2015, **134**, 317–324.
12. Bai, F. T., Sun, Y. H., Liu, Y. M. Thermogravimetric analysis of Huadian oil shale combustion at different oxygen concentrations. *Energ. Fuel.*, 2016, **30**(6), 4450–4456.
13. Xie, F. F., Wang, Z., Lin, W. G., Song, W. L. Study on thermal conversion of Huadian oil shale under N_2 and CO_2 atmospheres. *Oil Shale*, 2010, **27**(4), 309–320.
14. Ollero, P., Serrera, A., Arjona, R., Alcantarilla, S. Diffusional effects in TGA gasification experiments for kinetic determination. *Fuel*, 2002, **81**(15), 1989–2000.
15. Wang, Q., Jia, C., Jiang, Q., Wang, Y., Wu, D. Combustion characteristics of Indonesian oil sands. *Fuel Process. Technol.*, 2012, **99**, 110–114.
16. Akahira, T., Sunose, T. Method of determining activation deterioration constant of electrical insulating materials. *Res. Rep. Chiba Inst. Technol. (Sci. Technol.)*, 1971, **16**, 22–31.
17. Friedman, H. L. Kinetics of thermal degradation of char-forming plastics from thermogravimetry. Application to a phenolic plastic. *J. Polymer Sci. Pol. Sym.*, 1964, **6**(1), 183–195.
18. Bai, F. T., Sun, Y. H., Liu, Y. M., Li, Q., Guo, M. Y. Thermal and kinetic characteristics of pyrolysis and combustion of three oil shales. *Energ. Convers. Manage.*, 2015, **97**, 374–381.
19. Vyazovkin, S., Burnham, A. K., Criado, J. M., Pérez-Maqueda, L. A., Popescu, C., Sbirrazzuoli, N. ICTAC Kinetics Committee recommendations for performing kinetic computations on thermal analysis data. *Thermochim. Acta*, 2011, **520**(1–2), 1–19.
20. Bai, F. T., Guo, W., Lü, X. S., Liu, Y. M., Guo, M. Y., Li, Q., Sun, Y. H. Kinetic study on the pyrolysis behavior of Huadian oil shale via non-isothermal thermogravimetric data. *Fuel*, 2015, **146**, 111–118.
21. Sun, Y. H., Bai, F. T., Lü, X. S., Jia, C. X., Wang, Q., Guo, M. Y., Li, Q., Guo, W. Kinetic study of Huadian oil shale combustion using a multi-stage parallel reaction model. *Energy*, 2015, **82**, 705–713.
22. Chen, C. X., Ma, X. Q., Liu, K. Thermogravimetric analysis of microalgae combustion under different oxygen supply concentrations. *Appl. Energ.*, 2011, **88**(9), 3189–3196.
23. Fang, M. X., Shen, D. K, Li, Y. X., Yu, C. J., Luo, Z. Y., Cen, K. F. Kinetic study on pyrolysis and combustion of wood under different oxygen concentrations by using TG-FTIR analysis. *J. Anal. Appl. Pyrol.*, 2006, **77**(1), 22–27.
24. Li, S., Cheng, Y. Catalytic gasification of gas-coal char in CO_2. *Fuel*, 1995, **74**(3), 456–458.
25. Burnham, A. K. Reaction kinetics between CO_2 and oil-shale residual carbon. 2. Partial-pressure and catalytic-mineral effects. *Fuel*, 1979, **58**(10), 713–718.
26. Su, D. S., Müller, J.-O., Jentoft, R. E., Rothe, D., Jacob, E., Schlögl, R. Fullerene-like soot from EuroIV diesel engine: consequences for catalytic automotive pollution control. *Top. Catal.*, 2004, **30**(1–4)**,** 241–245.
27. Al-Makhadmeh, L., Maier, J., Al-Harahsheh, M., Scheffknecht, G. Oxy-fuel technology: An experimental investigation into oil shale combustion under oxy-fuel conditions. *Fuel*, 2013, **103**, 421–429.

28. Al-Makhadmeh, L. A., Maier, J., Batiha, M. A., Scheffknecht, G. Oxyfuel technology: Oil shale desulfurization behavior during staged combustion. *Fuel*, 2017, **190**, 229–236.

Presented by A. Siirde
Received December 28, 2017